Fronto-Striatal Dynamic Connectivity is linked to Dopaminergic Motor Response in Parkinson's Disease

Lukas Hensel MD[a,b], Aline Seger MD[a,b], Ezequiel Farrher PhD[c], Anna K. Bonkhoff MD[d], N. Jon Shah PhD[c,e,f], Gereon R. Fink MD[a,b], Christian Grefkes MD[g], Michael Sommerauer MD[a,b], Christopher E. J. Doppler MD[a,b]

[a]University of Cologne, Faculty of Medicine and University Hospital Cologne, Department of Neurology, 50937 Köln, Germany

[b]Cognitive Neuroscience, Institute of Neuroscience and Medicine (INM-3), Forschungszentrum Jülich, 52425 Jülich, Germany

[c]Institute of Neuroscience and Medicine 4 and Molecular Neuroscience and Neuroimaging (INM-4 / INM-11), Forschungszentrum Jülich, 52425 Jülich, Germany

[d]J. Philip Kistler Stroke Research Center, Massachusetts General Hospital, Harvard Medical School, Boston, United States

[e]JARA – BRAIN - Translational Medicine, 52056 Aachen, Germany

[f]RWTH Aachen University, Department of Neurology, 52056 Aachen, Germany

[g]University Hospital Frankfurt, Goethe University, Department of Neurology, Frankfurt am Main, Germany

Correspondence to: Christopher Doppler

Department of Neurology, University of Cologne, Cologne, Germany

E-mail: christopher.doppler@uk-koeln.de

Running title: connectivity-related Dopa-response

Keywords: Parkinson’s Disease, Dopamine, Levodopa, resting-state, dynamic functional connectivity

Abstract

Introduction: Differences in dopaminergic motor response in Parkinson's disease (PD) patients can be related to PD subtypes, and previous fMRI studies associated dopaminergic motor response with corticostriatal functional connectivity. While traditional fMRI analyses have assessed the mean connectivity between regions of interest, an important aspect driving dopaminergic response might lie in the temporal dynamics in corticostriatal connections.

Methods: This study aims to determine if altered resting-state dynamic functional network connectivity (DFC) is associated with dopaminergic motor response. To test this, static and DFC were assessed in 32 PD patients and 18 healthy controls (HC). Patients were grouped as low and high responders using a median split of their dopaminergic motor response.

Results: Patients featuring a high dopaminergic response were observed to spend more time in a regionally integrated state compared to HC. Furthermore, DFC between the anterior midcingulate cortex/dorsal anterior cingulate cortex (aMCC/dACC) and putamen was lower in low responders during a more segregated state and correlated with dopaminergic motor response.

Conclusion: The findings of this study revealed that temporal dynamics of fronto-striatal connectivity are associated with clinically relevant information, which may be considered when assessing functional connectivity between regions involved in motor initiation.

Introduction

Parkinson's disease (PD) is characterized by striatal dopaminergic depletion due to α-synucleinopathy-induced neurodegeneration. Even though a substantial response to dopaminergic therapy is frequent in PD, its absence does not exclude PD [1]. While this treatment-response variability has been corroborated in autopsy-proven PD cases [1,2], its underlying mechanisms remain poorly understood. Previous resting-state functional magnetic resonance imaging (rs-fMRI) investigations have suggested that higher functional connectivity of the striatum with remote cortical motor centers facilitates dopaminergic response [3–5]. These studies measured the mean connectivity over an entire scan session, i.e., several minutes (static connectivity).

Yet, dopaminergic signaling of these regions has been shown to occur in shorter temporal resolution, which may not be detected by traditional static connectivity analyses. Dopaminergic stimulation combined with microelectrode recordings in mice revealed a rapid dopaminergic response in the striatum on the scale of milliseconds, whereas neuron populations of the medial prefrontal cortex responded in a longer lasting, neuromodulatory effect over multiple seconds [6]. Given that medial prefrontal regions including the dorsal anterior cingulate cortex play a critical role in shifting between distinct large scale networks [7,8], the dopaminergic modulation of these regions likely involves time-sensitive connectivity patterns with distant brain regions. The effect of a dopaminergic replacement therapy on motor behavior hence likely involves transient network configurations, which may have been overlooked by traditional static connectivity measures. Assessing dynamic functional connectivity (DFC) from fMRI timeseries allows for detecting transient changes of connectivity within seconds, providing a more detailed picture of the brain's physiology in health and disease [9]. Even though these configurations are transient in nature, they might represent a persistent pattern of brain network functions.

Notably, such short-lasting connectivity patterns show abnormalities in several neurological disorders including Alzheimer's Disease and Parkinson's disease [10–14]. For example, recent studies could link changes in DFC with PD in [11,15], but also specifically with cognitive impairment and higher non-motor burden – including REM sleep behavior disorder [16] and depression [17] - in PD [11,14,18–20], suggesting distinct connectivity patterns for PD subtypes [13]. Regarding therapy-specific symptoms, changes in DFC could also be detected in PD patients with impulse control disorders [21].

We, therefore, investigated the association of DFC and the clinical improvement of motor function during dopamine replacement therapy in PD patients, comparing DFC between patients with low and high treatment responses. We computed DFC between cortical networks involved in primary sensorimotor function and motor initiation as well as subcortical networks comprising the basal ganglia and the cerebellum. Given the distribution of dopaminergic output trajectories, we expected differences in dynamic connectivity particularly in the striatum as well as medial prefrontal regions of interest.

Materials and methods

Participants

Thirty-two PD patients, diagnosed according to the current Movement Disorder Society (MDS) clinical diagnostic criteria [22] (25 with clinically established PD and 7 with clinically probable PD), and 18 healthy age- and sex-matched controls underwent anatomical MRI and rs-fMRI. Inclusion criteria were age between 51 - 80 years, geriatric depression scale (GDS-15) < 5, and Montreal cognitive assessment (MoCA) score > 22. Exclusion criteria encompassed contraindications for MRI, and – for patients – a motor symptom duration > 15 years. 25 patients met criteria for clinically established and 7 patients for clinically probable PD [22]. Motor deficits were assessed using the MDS Unified Parkinson's Disease Rating Scale part III (MDS-UPDRS III) during patients' regular medication (ON) and in the practical OFF state after 12 hours without dopaminergic medication overnight. To do this, we visited patients at their homes or in a hotel following an overnight stay. Once the MDS-UPDRS III examination was completed, patients were allowed to resume their regular medication. Patients typically spent three hours at the research center, and if they confirmed being in a personally accurate motor state, the MDS-UPDRS III examination for medication ON was repeated. None of the patients reported significant fluctuations, indicating that the medication ON remained relatively stable throughout the day. In order to determine the dopaminergic treatment response, the ratio of the MDS-UPDRS III between medication ON and OFF was calculated (i.e., *(([score during OFF] – [score during ON]) / score during OFF) * 100*). To differentiate tremor- and bradykinesia-related symptoms, we computed a tremor subscore (10 items: UPDRS 3.15-17) as well as a bradykinesia subscore (16 items: UPDRS 3.3-8 and 3.14). Patients were grouped using a median split of the response to dopaminergic therapy, distinguishing low and high responders (median = 26%, Figure 1). Additionally, we recorded motor symptom duration, Hoehn and Yahr stage, and levodopa equivalent daily doses (LEDD) [23].

Cognition was assessed as recommended in the MDS diagnostic criteria for mild cognitive impairment in Parkinson's disease [24]. Tests included the Verbal Learning and Memory Test and the Rey-Osterrieth Complex Figure Test for the memory domain; Trail Making test, digit span, and Stroop color and word test for working memory; phonemic verbal fluency (-s version), semantic verbal fluency (animals), and Trail Making Test for executive functioning; similarities from the German version of the Wechsler Adult Intelligence Scale, and Aphasia-Check-List for language abilities; Benton judgement of line orientation, and Rey-Osterrieth Complex Figure Test for visuospatial function. Z-scores for each cognitive domain were

calculated based on published age-corrected norms, if available, and from an in-house cohort of healthy subjects matched for age. A composite score of the average of the five domains' z-scores was calculated to estimate global cognitive performance.

The study was approved by the local ethics committee and all study participants gave written informed consent according to the Declaration of Helsinki.

Magnetic resonance image acquisition

Magnetic resonance images were acquired using a Siemens Trio 3T MR scanner. For rs-fMRI, participants were instructed to close their eyes and let their minds wander. Patients were instructed not to fall asleep, which was verified upon the end of the scan. An echo planar imaging (EPI) sequence comprising 300 volumes was utilized with the following parameters: repetition-time (TR) = 2200 ms, echo-time (TE) = 30 ms, field-of-view (FoV) = 200×200 mm^2, 36 axial slices, 3.1 mm^3 isotropic voxel-size, flip-angle = 90°. Additionally, T1-images were acquired (MP-RAGE, TR = 2.5 s, TE = 2.89 ms, FoV = 256×256 mm^2, 176 axial slices, 1 mm^3 isotropic voxel-size, flip-angle = 7°) to screen for structural abnormalities.

Resting-State fMRI Preprocessing

Rs-fMRI data were preprocessed using Statistical Parametric Mapping (SPM12; Wellcome Centre for Human Neuroimaging, London, UK) implemented in Matlab version 2019b (Mathworks Inc.; MA, USA). Distortion correction was performed using FSL (FMRIB Software Library v6.0; https://fsl.fmrib.ox.ac.uk/fsl/fslwiki/FSL). The first five EPI volumes were discarded, avoiding noise from magnetic field saturation. The remaining 295 volumes were corrected for head movements by spatial realignment to the mean image, normalized into MNI space using the unified segmentation approach [25], and smoothed with a Gaussian filter of 8 mm full-width-at-half-maximum.

Static and Dynamic Connectivity

Functional connectivity was extracted using the GIFT toolbox (version 4.0, https://trendscenter.org/software/gift/), as implemented in SPM. First, we used an independent component analysis (ICA), constrained by components from rs-fMRI data of 405 healthy controls (HC) [26,27], to extract spatially distinct intrinsic components [28,29]. From these components, ten volumes-of-interest (VOIs) were selected, contributing to four key motor systems [30], namely the sensorimotor network, the motor initiation network, the basal ganglia

network, and the cerebellar network (Figure 2 A). For artifact removal, components' time courses were detrended, despiked using 3Ddespike [31], filtered by a fifth-order Butterworth low-pass filter (cut-off: 0.15 Hz), and normalized for variance [32]. Static connectivity between VOIs was assessed by computing mean Pearson's pairwise and Fisher z-transformed correlations. DFC between the same VOIs was performed by applying the sliding window approach [26,33–35] in steps of one TR using a window size of 44 s and a Gaussian window alpha of three. Within each window, DFC was estimated from the l_1-regularized precision matrix. Age, sex, mean framewise translation and rotation were regressed out as covariates of no interest. As for static connectivity, all matrices resulting from the DFC analysis were Fisher z-transformed. Matrices from all participants were finally entered into a k-means clustering analysis, grouping re-occurring connectivity patterns [26,34,36]. The similarity of each window's connectivity to the cluster centroid was estimated using the l1 distance (Manhattan distance). An optimal clustering solution of k = 2 was indicated by the silhouette measure [37] and elbow criterion [38].

Statistics

We performed statistical data analyses using python (Version 3.8), including the 'SciPy' package [39]. To measure the dynamic shifts between connectivity states, we assessed dwell times (i.e., the mean time in one state without transitioning to another), fraction times (i.e., the portion of total time in one state), and the number of transitions between states. Differences between these measures were compared by three-level one-way analyses of variance (ANOVAs) testing for group differences between the three groups: HC, and PD patients with low and high responses to dopaminergic therapy. Further, we provide a comparison of these measures between all patients and controls using independent t-tests in the supplementary material to grant compatibility to future DFC studies.

Likewise, we tested for group differences in connectivity pairs (static and dynamic), using three-level one-way ANOVAs for each connection (significance level P = 0.05, FDR-corrected).

Results

Participants

Demographic and clinical information is summarized in Table 1. Subgroups with low or high response to dopaminergic therapy did not differ in age, sex, motor symptom severity, cognitive impairment, LEDD, or within-scanner head motion. An overview of individual ON and OFF scores is illustrated in Figure 1, differentiating bradykinesia- and tremor-related subscores of UPDRS III items. Detailed results for each cognitive domain (memory, working memory, executive function, language, and visuospatial function) are provided in the supplementary material (Table S2). Importantly, no significant differences were found between groups.

Static and Dynamic Connectivity

Static functional connectivity across all participants showed positive connectivity within cortical, basal ganglia, and cerebellar networks but negative connectivity between cortical and subcortical networks (Figure 2 B). This connectivity pattern is in line with previous rs-fMRI studies on PD [13,14,40]. FDR-corrected ANOVAs for *static* connectivity pairs did not show significant group differences. Regarding dynamic functional connectivity (DFC), we found two states, which essentially differed in their within- and between-network connectivity. Both states (Figure 2 B) featured positive within-network connectivity and negative between-network connectivity in cortical and subcortical networks. However, this modular organization was less pronounced in state 1, showing most positive connections within cortical, basal ganglia and cerebellar networks. In contrast, state 2 was marked by highly negative connections, segregating cortical regions from subcortical and cerebellar regions. Comparing dwell times between groups revealed that patients with high response to dopaminergic therapy spent significantly more time in state 1, compared to HC (three-level one-way ANOVA: $P = 0.010$, *post-hoc* independent t-tests: $t(32) = 3.3$, $P = 0.002$, Figure 2 C). Dwell times for state 2 did not differ significantly between groups (Figure 2 C). No significant differences were found for fraction times ($P = 0.090$) and number of transitions ($P = 0.216$). As shown in the group comparison between all patients and HC presented in the supplementary material, significant differences of dwell times as well as fraction times could be found independently from treatment response subgroups. Hence, the significant main effect of group of the ANOVA between dwell times of HC, low and high responding patients indicates that specifically a prolonged maintenance of state 1 was associated with a high dopaminergic response. In contrast, fraction times summarizing the total of short and long episodes in this state, was observed in PD more generally, not significantly interacting with dopaminergic response.

Connectivity related to treatment effect

Furthermore, FDR-corrected ANOVAs indicated that DFC between aMCC/dACC and putamen was significantly lower in patients with a low response to dopaminergic therapy during state 2 and correlated with the effect of dopaminergic treatment on motor performance (Figure 2 D). To challenge whether the association of this functional connection and dopaminergic response was driven by the severity of motor symptoms or amount of dopaminergic medication, we tested Pearson correlations between aMCC/dACC-putamen connectivity and the UPDRS III OFF medication as well as LEDD. Neither of both tests showed a significant correlation with aMCC/dACC-putamen connectivity (UPDRSIII OFF: *Pearson R* = 0.11, *P* = 0.595; LEDD: *Pearson R* = 0.26, *P* = 0.211). Further, including LEDD and the UPDRS III OFF scores as covariates resulted in a significant partial correlation between dopaminergic response and aMCC/dACC-putamen connectivity (*Pearson R* = 0.56, *P* = 0.007). These findings suggest that the observed reduction of fronto-striatal connectivity was associated with responsiveness to dopaminergic treatment rather than the motor symptoms or dopaminergic modulation *per se*.

Discussion

The present study links dynamic connectivity patterns and patients' responses to dopaminergic therapy, which could not be detected by a comparable static connectivity analysis. Specifically, the subgroup of patients with a high response to dopaminergic therapy spent more time in a state featuring lower within-network connectivity but higher connectivity between networks (i.e., between cortical and striatal regions) – in other words, a more integrated brain state. The predominance of this state in PD patients with a high dopaminergic treatment effect suggests that engagement of non-striatal and non-dopaminergic networks may be involved in a more significant treatment response. This finding may be interpreted in the framework of large-scale functional network organization [41–43], balancing between functional segregation and integration to enable optimal information processing. In this sense, a more segregated organization of neuronal populations promotes local information exchange, whereas a more integrative organization enhances information exchange between domains. The present findings show that high responders show prolonged information processing in a more integrative connectivity state, marked by less isolated within-domain connectivity (Figure 2 C). Our study extends findings by Kim et al. [11], who showed that PD patients in general spent more time in a more segregated state, by indicating the same pattern particularly for

high responders as a subgroup of PD patients. Previous DFC studies in PD associated a similar shift towards states with higher cortico-striatal integration with better cognitive [13,14] and motor [13] function, indicating an association between such a DFC fingerprint and a more benign PD phenotype. Similar to previous studies on differences in DFC associated with non-motor symptoms [16,17,19,20] and therapy-related effects [21] of PD patients, our data suggest that dopaminergic motor response is associated with specific dynamic connectivity patterns in the motor circuitry.

Similar relationships between better clinical performance and network integration have been observed in other disease entities including stroke [44,45] and traumatic brain injury [46]. These observations have led to the hypothesis that disturbed brain networks promote a more isolated within-network processing, which may be less prone to erroneous interactions with other domains [44]. With regards to PD, our findings suggest that a more integrated (thereby less segregated) connectivity between prefrontal regions involved in movement initiation, sensorimotor regions and the basal ganglia contributes to an enhanced propagation of dopaminergic treatment effects across brain networks. In line with this interpretation, patients with a *low* response to dopaminergic therapy expressed more negative connectivity between aMCC/dACC and putamen in the more segregated state 2, compared to HC and high responders (Figure 2 D). This connection is a crucial part of dopaminergic cortico-striatal loops involved in motivation and motor initiation [4,5,47] and was previously found to feature reduced functional connectivity in PD [40].

Assessing static functional connectivity in a sample of 19 patients with advanced PD (disease duration 4-22y), Akram and colleagues reported a similar correlation between the improvement of motor symptoms and fronto-striatal connectivity [5]. While static connectivity was unable to detect such a relationship in our sample, our findings suggest that a transiently reduced cortico-striatal integration involving the aMCC/dACC critically relates to the motor improvement induced by dopamine replacement therapy.

As a limitation, we acquired imaging data under dopaminergic treatment (medication ON) only. Consequently, we cannot distinguish whether 1) the negative connectivity between aMCC/dACC and putamen in low responders reflects an insufficient dopaminergic up-regulation of cortico-striatal loops correlating with the clinical response across patients, or 2) reflects a functional network alteration with a lacking cortico-striatal integration, which may be already observed in the OFF state, leading to the low dopaminergic effect. Hence, while the present study does not allow describing which connectivity patterns are directly altered by dopaminergic treatment, it demonstrates that the motor system under dopaminergic therapy features distinct DFC in patients with higher compared to lower treatment success. It would be interesting to investigate DFC in PD patients both in the medication ON and OFF condition, thus enabling a comprehensive examination of potential alterations in DFC between these two

conditions. However, the disadvantages of scanning in the medication OFF state, such as reduced comfort for patients and potentially increased motion artifacts, need to be taken into consideration. Notably, most patients in our cohort would not have been able to perform an MRI scan in their OFF state. Further, we did not perform a standardized levodopa challenge to formally measure the levodopa response. While we cannot rule out the potential influence of different treatment regimens, motor symptoms under regular dopaminergic treatment is assumed to give a realistic estimate of the patient's individual treatment effect. Even though some patients exhibited only a mild treatment effect, all patients fulfilled the MDS clinical diagnostic criteria for PD. Specifically, in those patients with a treatment effect of less than 30 % a clear response to dopaminergic therapy was evident and documented in the patient's history.

To conclude, the present data demonstrate an association between treatment response in PD and the temporal dynamics of fronto-striatal connections. Such dopamine sensitive connectivity patterns could be detected when assessing dynamic, but not static functional connectivity, indicating that temporally variable brain states contain valuable information on the integrity of dopaminergic systems for motor initiation in PD.

Contributions

1. Research project: A. Conception, B. Organization, C. Execution;
2. Statistical Analysis: A. Design, B. Execution, C. Review and Critique;
3. Manuscript Preparation: A. Writing of the first draft, B. Review and Critique;

LH: 1A, 2A, 2B, 3A

AS: 1B, 1C, 3B

EF: 1C, 3B

AKB: 2C, 3B

NJS: 3B

GRF: 1A, 3B

CG: 2A, 3B

MS: 1A, 1B, 2C, 3B

CEJD: 1A, 1B, 2B, 3A

Funding

LH, CG, and GRF are funded by the Deutsche Forschungsgemeinschaft (DFG, German Research Foundation) – Project-ID 431549029 – SFB 1451 (project C05).

MS is funded by the Koeln Fortune Program / Faculty of Medicine, University of Cologne (grant number 453/2018), and the Else Kröner-Fresenius-Stiftung (grant number 2019_EKES.02). MS is receiving funding from the program "Netzwerke 2021", an initiative of the Ministry of Culture and Science of the State of Northrhine Westphalia.

CEJD is supported by the Clinician Scientist Program (CCSP) / Faculty of Medicine / University of Cologne, funded by the Deutsche Forschungsgemeinschaft (DFG, German Research Foundation, FI 773/15-1)

The authors declare that there are no additional financial disclosures to report.

Competing interests

The authors report no competing interests.

Figure captions

Figure 1: Individual MDS-UPDRS III scores of low and high responder Parkinson's disease patients differentiating subscores of bradykinesia- (purple), and tremor-related (green) and axial or speech symptom-related (grey) subitems ON (light) and OFF (dark) medication. Relative responses to dopaminergic treatment (percentage change between OFF and ON) are provided on the x-axis. The median change in MDS-UPDRS III score related to dopaminergic therapy (black vertical line) was used as cut-off between the two groups (low responders and high responders). Abbreviation: UPDRS = MDS Unified Parkinson's Disease Rating Scale part III.

Figure 2: (A) Spatial ICA components across Parkinson's disease patients and HC superimposed on brain renderings and allocated to color-coded networks: MIN (dark purple) = motor initiation network, SMN (light blue) = sensorimotor network, BG (dark green) = basal ganglia, CB (light green) = cerebellum.

(B) Connectivity matrices across all HC and Parkinson's disease patients indicating low (red) and high (blue) connectivity showing positive within-network connectivity and negative between-network connectivity in cortical and subcortical networks. The colored bars at the top and the left side refer to the respective color-coded networks introduced in section A. The asterisk indicates significant group differences (FDR-corrected ANOVAs) **(C)** ANOVA results of dwell times showing that high responders spent more time than HC in state 1 before changing to state 2. **(D)** The association between aMCC/dACC-putamen connectivity in state 2 and response to dopaminergic therapy is demonstrated by a positive Pearson correlation (left) and significant group differences (right), indicating lower connectivity of low responders, than high responders and HC.
Abbreviations: dFNC = dynamic functional connectivity, HC = healthy controls, ICA = independent component analysis, LR = low responders, HR = high responders. DLPFC = dorsolateral prefrontal cortex, SMA = supplementary motor area, aMCC/dACC = anterior midcingulate cortex/ dorsal anterior cingulate cortex, S1/M1 = primary sensorimotor cortex, dPMC = dorsal premotor cortex.

References

[1] W.R.W. Martin, M. Miles, Q. Zhong, J. Hartlein, B.A. Racette, S.A. Norris, M. Ushe, B. Maiti, S. Criswell, A.A. Davis, P.T. Kotzbauer, N.J. Cairns, R.J. Perrin, J.S. Perlmutter, Is Levodopa Response a Valid Indicator of Parkinson's Disease?, Movement Disord. 36 (2021) 948–954. https://doi.org/10.1002/mds.28406.

[2] A.J. Hughes, S.E. Daniel, S. Blankson, A.J. Lees, A Clinicopathologic Study of 100 Cases of Parkinson's Disease, Arch Neurol-Chicago. 50 (1993) 140–148. https://doi.org/10.1001/archneur.1993.00540020018011.

[3] M. Tahmasian, L.M. Bettray, T. van Eimeren, A. Drzezga, L. Timmermann, C.R. Eickhoff, S.B. Eickhoff, C. Eggers, A systematic review on the applications of resting-state fMRI in Parkinson's disease: Does dopamine replacement therapy play a role?, Cortex; a Journal Devoted to the Study of the Nervous System and Behavior. 73 (2015) 80–105. https://doi.org/10.1016/j.cortex.2015.08.005.

[4] D.M. Cole, C.F. Beckmann, N.Y.L. Oei, S. Both, J.M.A. van Gerven, S.A.R.B. Rombouts, Differential and distributed effects of dopamine neuromodulations on resting-state network connectivity, Neuroimage. 78 (2013) 59–67. https://doi.org/10.1016/j.neuroimage.2013.04.034.

[5] H. Akram, C. Wu, J. Hyam, T. Foltynie, P. Limousin, E. Vita, T. Yousry, M. Jahanshahi, M. Hariz, T. Behrens, J. Ashburner, L. Zrinzo, l-Dopa responsiveness is associated with distinctive connectivity patterns in advanced Parkinson's disease, Movement Disord. 32 (2017) 874–883. https://doi.org/10.1002/mds.27017.

[6] Z.R. Holloway, T.G. Freels, J.F. Comstock, H.G. Nolen, H.J. Sable, D.B. Lester, Comparing phasic dopamine dynamics in the striatum, nucleus accumbens, amygdala, and medial prefrontal cortex, Synapse. 73 (2019) e22074. https://doi.org/10.1002/syn.22074.

[7] W.W. Seeley, V. Menon, A.F. Schatzberg, J. Keller, G.H. Glover, H. Kenna, A.L. Reiss, M.D. Greicius, Dissociable intrinsic connectivity networks for salience processing and

executive control., Journal of Neuroscience. 27 (2007) 2349–2356. https://doi.org/10.1523/jneurosci.5587-06.2007.

[8] W.W. Seeley, The Salience Network: A Neural System for Perceiving and Responding to Homeostatic Demands, J Neurosci. 39 (2019) 9878–9882. https://doi.org/10.1523/jneurosci.1138-17.2019.

[9] D.J. Lurie, D. Kessler, D.S. Bassett, R.F. Betzel, M. Breakspear, S. Kheilholz, A. Kucyi, R. Liégeois, M.A. Lindquist, A.R. McIntosh, R.A. Poldrack, J.M. Shine, W.H. Thompson, N.Z. Bielczyk, L. Douw, D. Kraft, R.L. Miller, M. Muthuraman, L. Pasquini, A. Razi, D. Vidaurre, H. Xie, V.D. Calhoun, Questions and controversies in the study of time-varying functional connectivity in resting fMRI, Netw Neurosci. 4 (2020) 30–69. https://doi.org/10.1162/netn_a_00116.

[10] D.T. Jones, P. Vemuri, M.C. Murphy, J.L. Gunter, M.L. Senjem, M.M. Machulda, S.A. Przybelski, B.E. Gregg, K. Kantarci, D.S. Knopman, B.F. Boeve, R.C. Petersen, C.R. Jack, Non-Stationarity in the "Resting Brain's" Modular Architecture, PLoS ONE. 7 (2012) e39731. https://doi.org/10.1371/journal.pone.0039731.

[11] J. Kim, M. Criaud, S.S. Cho, M. Díez-Cirarda, A. Mihaescu, S. Coakeley, C. Ghadery, M. Valli, M.F. Jacobs, S. Houle, A.P. Strafella, Abnormal intrinsic brain functional network dynamics in Parkinson's disease, Brain. 140 (2017) 2955–2967. https://doi.org/10.1093/brain/awx233.

[12] D. Cordes, X. Zhuang, M. Kaleem, K. Sreenivasan, Z. Yang, V. Mishra, S.J. Banks, B. Bluett, J.L. Cummings, Advances in functional magnetic resonance imaging data analysis methods using Empirical Mode Decomposition to investigate temporal changes in early Parkinson's disease, Alzheimer's Dement.: Transl. Res. Clin. Interv. 4 (2018) 372–386. https://doi.org/10.1016/j.trci.2018.04.009.

[13] M. Diez-Cirarda, I. Gabilondo, N. Ibarretxe-Bilbao, J.C. Gómez-Esteban, J. Kim, O. Lucas-Jiménez, R.D. Pino, J. Peña, N. Ojeda, A. Mihaescu, M. Valli, M.A. Acera, A. Cabrera-Zubizarreta, M.A. Gómez-Beldarrain, A.P. Strafella, Contributions of sex, depression, and cognition on brain connectivity dynamics in Parkinson's disease, Npj Park Dis. 7 (2021) 117. https://doi.org/10.1038/s41531-021-00257-9.

[14] E. Fiorenzato, A.P. Strafella, J. Kim, R. Schifano, L. Weis, A. Antonini, R. Biundo, Dynamic functional connectivity changes associated with dementia in Parkinson's disease., Brain. 142 (2019) 2860–2872. https://doi.org/10.1093/brain/awz192.

[15] F. Nieuwhof, R.C. Helmich, Entangled cerebral networks in Parkinson's disease, Brain. 140 (2017) 2767–2769. https://doi.org/10.1093/brain/awx267.

[16] C. Gan, K. Ma, L. Wang, Q. Si, M. Wang, Y. Yuan, K. Zhang, Dynamic functional connectivity changes in Parkinson's disease patients with REM sleep behavior disorder, Brain Res. 1764 (2021) 147477. https://doi.org/10.1016/j.brainres.2021.147477.

[17] J. Xu, M. Yu, H. Wang, Y. Li, L. Li, J. Ren, C. Pan, W. Liu, Altered Dynamic Functional Connectivity in de novo Parkinson's Disease Patients With Depression, Front. Aging Neurosci. 13 (2022) 789785. https://doi.org/10.3389/fnagi.2021.789785.

[18] T.M. Madhyastha, M.K. Askren, P. Boord, T.J. Grabowski, Dynamic Connectivity at Rest Predicts Attention Task Performance, Brain Connectivity. 5 (2015) 45–59. https://doi.org/10.1089/brain.2014.0248.

[19] Y. Cao, Q. Si, R. Tong, X. Zhang, C. Li, S. Mao, Abnormal dynamic functional connectivity changes correlated with non-motor symptoms of Parkinson's disease, Front. Neurosci. 17 (2023) 1116111. https://doi.org/10.3389/fnins.2023.1116111.

[20] G. Engels, A. Vlaar, B. McCoy, E. Scherder, L. Douw, Dynamic Functional Connectivity and Symptoms of Parkinson's Disease: A Resting-State fMRI Study, Front. Aging Neurosci. 10 (2018) 388. https://doi.org/10.3389/fnagi.2018.00388.

[21] I. Navalpotro-Gomez, J. Kim, P.M. Paz-Alonso, M. Delgado-Alvarado, A. Quiroga-Varela, H. Jimenez-Urbieta, M. Carreiras, A.P. Strafella, M.C. Rodriguez-Oroz, Disrupted salience network dynamics in Parkinson's disease patients with impulse control disorders, Park. Relat. Disord. 70 (2020) 74–81. https://doi.org/10.1016/j.parkreldis.2019.12.009.

[22] R.B. Postuma, D. Berg, M. Stern, W. Poewe, C.W. Olanow, W. Oertel, J. Obeso, K. Marek, I. Litvan, A.E. Lang, G. Halliday, C.G. Goetz, T. Gasser, B. Dubois, P. Chan, B.R. Bloem, C.H. Adler, G. Deuschl, MDS clinical diagnostic criteria for Parkinson's disease., Movement Disorders. 30 (2015) 1591–1601. https://doi.org/10.1002/mds.26424.

[23] C.L. Tomlinson, R. Stowe, S. Patel, C. Rick, R. Gray, C.E. Clarke, Systematic review of levodopa dose equivalency reporting in Parkinson's disease., Movement Disorders. 25 (2010) 2649–2653. https://doi.org/10.1002/mds.23429.

[24] I. Litvan, J.G. Goldman, A.I. Tröster, B.A. Schmand, D. Weintraub, R.C. Petersen, B. Mollenhauer, C.H. Adler, K. Marder, C.H. Williams-Gray, D. Aarsland, J. Kulisevsky, M.C. Rodriguez-Oroz, D.J. Burn, R.A. Barker, M. Emre, Diagnostic criteria for mild cognitive impairment in Parkinson's disease: Movement Disorder Society Task Force guidelines, Movement Disord. 27 (2012) 349–356. https://doi.org/10.1002/mds.24893.

[25] J. Ashburner, K.J. Friston, Unified segmentation., NeuroImage. 26 (2005) 839–851. https://doi.org/10.1016/j.neuroimage.2005.02.018.

[26] E.A. Allen, E. Damaraju, S.M. Plis, E.B. Erhardt, T. Eichele, V.D. Calhoun, Tracking Whole-Brain Connectivity Dynamics in the Resting State, Cereb Cortex. 24 (2014) 663–676. https://doi.org/10.1093/cercor/bhs352.

[27] V.D. Calhoun, T. Adali, G.D. Pearlson, J.J. Pekar, A method for making group inferences from functional MRI data using independent component analysis, Hum Brain Mapp. 14 (2001) 140–151. https://doi.org/10.1002/hbm.1048.

[28] Q. Lin, J. Liu, Y. Zheng, H. Liang, V.D. Calhoun, Semiblind spatial ICA of fMRI using spatial constraints, Hum Brain Mapp. 31 (2010) 1076–1088. https://doi.org/10.1002/hbm.20919.

[29] Y. Du, Y. Fan, Group information guided ICA for fMRI data analysis, Neuroimage. 69 (2013) 157–197. https://doi.org/10.1016/j.neuroimage.2012.11.008.

[30] D. Caligiore, R.C. Helmich, M. Hallett, A.A. Moustafa, L. Timmermann, I. Toni, G. Baldassarre, Parkinson's disease as a system-level disorder, Npj Park Dis. 2 (2016) 16025. https://doi.org/10.1038/npjparkd.2016.25.

[31] R.W. Cox, AFNI: Software for Analysis and Visualization of Functional Magnetic Resonance Neuroimages, Comput Biomed Res. 29 (1996) 162–173. https://doi.org/10.1006/cbmr.1996.0014.

[32] S. Rachakonda, Egolf, Correa, Calhoun, Group ICA of fMRI toolbox (GIFT) manual, (2007). file:///Users/lukashensel/Downloads/v1.3h_GIFTManual.pdf (accessed August 2, 2022).

[33] Ü. Sakoğlu, G.D. Pearlson, K.A. Kiehl, Y.M. Wang, A.M. Michael, V.D. Calhoun, A method for evaluating dynamic functional network connectivity and task-modulation: application to schizophrenia, Magnetic Reson Mater Phys Biology Medicine. 23 (2010) 351–366. https://doi.org/10.1007/s10334-010-0197-8.

[34] V.D. Calhoun, R. Miller, G. Pearlson, T. Adalı, The Chronnectome: Time-Varying Connectivity Networks as the Next Frontier in fMRI Data Discovery, Neuron. 84 (2014) 262–274. https://doi.org/10.1016/j.neuron.2014.10.015.

[35] E. Damaraju, E.A. Allen, A. Belger, J.M. Ford, S. McEwen, D.H. Mathalon, B.A. Mueller, G.D. Pearlson, S.G. Potkin, A. Preda, J.A. Turner, J.G. Vaidya, T.G. van Erp, V.D. Calhoun, Dynamic functional connectivity analysis reveals transient states of dysconnectivity in schizophrenia, Neuroimage Clin. 5 (2014) 298–308. https://doi.org/10.1016/j.nicl.2014.07.003.

[36] S. Lloyd, Least squares quantization in PCM, Ieee T Inform Theory. 28 (1982) 129–137. https://doi.org/10.1109/tit.1982.1056489.

[37] P.J. Rousseeuw, Silhouettes: A graphical aid to the interpretation and validation of cluster analysis, J Comput Appl Math. 20 (1987) 53–65. https://doi.org/10.1016/0377-0427(87)90125-7.

[38] F.A. Espinoza, J.A. Turner, V.M. Vergara, R.L. Miller, E. Mennigen, J. Liu, M.B. Misiura, J. Ciarochi, H.J. Johnson, J.D. Long, H.J. Bockholt, V.A. Magnotta, J.S. Paulsen, V.D. Calhoun, Whole-Brain Connectivity in a Large Study of Huntington's Disease Gene Mutation Carriers and Healthy Controls, Brain Connectivity. 8 (2018) 166–178. https://doi.org/10.1089/brain.2017.0538.

[39] P. Virtanen, R. Gommers, T.E. Oliphant, M. Haberland, T. Reddy, D. Cournapeau, E. Burovski, P. Peterson, W. Weckesser, J. Bright, S.J. van der Walt, M. Brett, J. Wilson, K.J. Millman, N. Mayorov, A.R.J. Nelson, E. Jones, R. Kern, E. Larson, C.J. Carey, İ. Polat, Y. Feng, E.W. Moore, J. VanderPlas, D. Laxalde, J. Perktold, R. Cimrman, I. Henriksen, E.A. Quintero, C.R. Harris, A.M. Archibald, A.H. Ribeiro, F. Pedregosa, P. van Mulbregt, S. 1 0 Contributors, A. Vijaykumar, A.P. Bardelli, A. Rothberg, A. Hilboll, A. Kloeckner, A. Scopatz, A. Lee, A. Rokem, C.N. Woods, C. Fulton, C. Masson, C. Häggström, C. Fitzgerald, D.A. Nicholson, D.R. Hagen, D.V. Pasechnik, E. Olivetti, E. Martin, E. Wieser, F. Silva, F. Lenders, F. Wilhelm, G. Young, G.A. Price, G.-L. Ingold, G.E. Allen, G.R. Lee, H. Audren, I. Probst, J.P. Dietrich, J. Silterra, J.T. Webber, J. Slavič, J. Nothman, J. Buchner, J. Kulick, J.L. Schönberger, J.V. de M. Cardoso, J. Reimer, J. Harrington, J.L.C. Rodríguez, J. Nunez-Iglesias, J. Kuczynski, K. Tritz, M. Thoma, M. Newville, M. Kümmerer, M. Bolingbroke, M. Tartre, M. Pak, N.J. Smith, N. Nowaczyk, N. Shebanov, O. Pavlyk, P.A. Brodtkorb, P. Lee, R.T. McGibbon, R. Feldbauer, S. Lewis, S. Tygier, S. Sievert, S. Vigna, S. Peterson, S. More, T. Pudlik, T. Oshima, T.J. Pingel, T.P. Robitaille, T. Spura, T.R. Jones, T. Cera, T. Leslie, T. Zito, T. Krauss, U. Upadhyay, Y.O. Halchenko, Y. Vázquez-Baeza, SciPy 1.0: fundamental algorithms for scientific computing in Python, Nat Methods. 17 (2020) 261–272. https://doi.org/10.1038/s41592-019-0686-2.

[40] L. Hensel, F. Hoffstaedter, J. Caspers, J. Michely, C. Mathys, J. Heller, C.R. Eickhoff, K. Reetz, M. Südmeyer, G.R. Fink, A. Schnitzler, C. Grefkes, S.B. Eickhoff, Functional Connectivity Changes of Key Regions for Motor Initiation in Parkinson's Disease, Cerebral Cortex (New York, N.Y. : 1991). 29 (2018) 383–396. https://doi.org/10.1093/cercor/bhy259.

[41] O. Sporns, Network attributes for segregation and integration in the human brain, Curr Opin Neurobiol. 23 (2013) 162–171. https://doi.org/10.1016/j.conb.2012.11.015.

[42] K.J. Friston, Functional and effective connectivity: a review., Brain Connectivity. 1 (2011) 13–36. https://doi.org/10.1089/brain.2011.0008.

[43] S.B. Eickhoff, C. Grefkes, Approaches for the Integrated Analysis of Structure, Function and Connectivity of the Human Brain, Clin Eeg Neurosci. 42 (2011) 107–121. https://doi.org/10.1177/155005941104200211.

[44] A.K. Bonkhoff, F.A. Espinoza, H. Gazula, V.M. Vergara, L. Hensel, J. Michely, T. Paul, A.K. Rehme, L.J. Volz, G.R. Fink, V.D. Calhoun, C. Grefkes, Acute ischaemic stroke alters the brain's preference for distinct dynamic connectivity states., Brain. 143 (2020) 1525–1540. https://doi.org/10.1093/brain/awaa101.

[45] A.K. Bonkhoff, A.K. Rehme, L. Hensel, C. Tscherpel, L.J. Volz, F.A. Espinoza, H. Gazula, V.M. Vergara, G.R. Fink, V.D. Calhoun, N.S. Rost, C. Grefkes, Dynamic connectivity predicts acute motor impairment and recovery post-stroke., Brain Commun. 3 (2021) fcab227. https://doi.org/10.1093/braincomms/fcab227.

[46] A.F. Kuceyeski, K.W. Jamison, J.P. Owen, A. Raj, P. Mukherjee, Longitudinal increases in structural connectome segregation and functional connectome integration are associated with better recovery after mild TBI, Hum Brain Mapp. 40 (2019) 4441–4456. https://doi.org/10.1002/hbm.24713.

[47] S.N. Haber, The place of dopamine in the cortico-basal ganglia circuit, Neuroscience. 282 (2014) 248–257. https://doi.org/10.1016/j.neuroscience.2014.10.008.

Table 1

	HC (n = 18)	PD LR (n = 16)	PD HR (n = 16)	P
Age [y]	67.6 ± 7.7	66.6 ± 8.4	65.8 ± 7.0	0.784[1]
Sex [m/f]	13/5	10/6	14/2	0.274[2]
Hoehn & Yahr stage*		2.00 (2.00 - 2.25)	2.00 (2.00 - 2.63)	0.616[4]
Motor symptom duration [y]		4.9 ± 3.2	6.0 ± 3.3	0.346[3]
MDS-UPDRS III (ON)*		29.00 (18.00 - 36.25)	26.00 (18.00 - 28.25)	0.432[4]
MDS-UPDRS III (OFF)*		35.00 (21.75 - 42.25)	42.50 (27.75 – 51.00)	0.160[4]
Bradykinesia Subscore (ON)		16.00 (10.25 - 22.25)	14.50 (9.00 - 18.00)	0.780[4]
Bradykinesia Subscore (OFF)		19.50 (9.25 - 24.00)	25.5 (18.75 - 30.25)	0.138[4]
Bradykinesia response [%]		10.93 ± 16.34	40.30 ± 13.05	<0.001[3]
Tremor Subscore (ON)		7.00 (3.00 - 11.50)	6.50 (2.75 - 7.25)	0.361[4]
Tremor Subscore (OFF)		10.00 (3.75 - 12.25)	8.00 (6.75 - 11.25)	0.724[4]
Tremor response [%]		14.46 ± 21.60	35.61 ± 34.59	0.047[3]
LEDD (total)		442.5 ± 259.8	659.6 ± 480.0	0.120[3]
LEDD (levodopa only)		257.8 ± 176.7	381.3 ± 249.2	0.117[3]
LEDD (levodopa and COMT inhibitors)		272.7 ± 204.0	441.3 ± 367.4	0.119[3]
LEDD (only dopamine agonists)		126.1 ± 106.2	149.6 ± 117.9	0.558[3]
LEDD (only MAO-B inhibitors)		31.3 ± 47.9	43.8 ± 51.2	0.481[3]
Patients on levodopa		12/16 (75 %)	14/16 (87,5 %)	0.365[5]
Patients on dopamine agonists		11/16 (68,8 %)	12/16 (75 %)	0.694[5]

MDS criteria established/ probable		11/5	14/2	0.200[5]
GDS-15*	0.50 (0.00 - 1.00)	1.00 (0.00 - 2.00)	0.00 (0.00 - 1.25)	0.258[2]
MoCA*	27.00 (26.00 - 27.00)	26.50 (25.75 - 29.00)	27.50 (25.00 - 28.00)	0.894[2]
NPT [z-score]	0.17 ± 0.47	0.33 ± 0.43	0.25 ± 0.46	0.628[1]
Rotation [degrees]	0.0022 ± 0.0013	0.0021 ± 0.0007	0.0031 ± 0.0022	0.150[1]
Translation [mm]	0.26 ± 0.08	0.25 ± 0.12	0.29 ± 0.10	0.480[1]
MFWD [mm]	0.26	0.26 ± 0.12	0.30 ± 0.10	0.470[1]

Table 1: Demographics, clinical and MRI characteristics in healthy controls (HC) and Parkinson's disease patients with low (LR) and high (HR) response to dopaminergic therapy.
Abbreviations: COMT = catechol-O-methyltransferase, GDS-15 = Geriatric Depression Scale, HC = healthy controls, HR = high response to dopaminergic therapy, LEDD = levodopa daily equivalent dose, LR = low response to dopaminergic therapy, MAO-B = monoamino oxidase type B, MDS-UPDRS III = Movement Disorder Society Unified Parkinson's Disease Rating Scale part III, MoCA = Montreal Cognitive Assessment, NPT = Neuropsychological testing, PD = Parkinson's disease, MFWD = Mean Framewise Displacement, * = ordinal data is described by medians and interquartile range between first and third quartiles, instead of means and standard deviations. [1]ANOVA (HC vs. PD LR vs. PD HR), [2]H-test (HC vs. PD LR vs. PD HR), [3]t-test (PD LR vs. PD HR), [4]U-test (PD LR vs. PD HR), [5]chi-square-test (PD LR vs. PD HR).

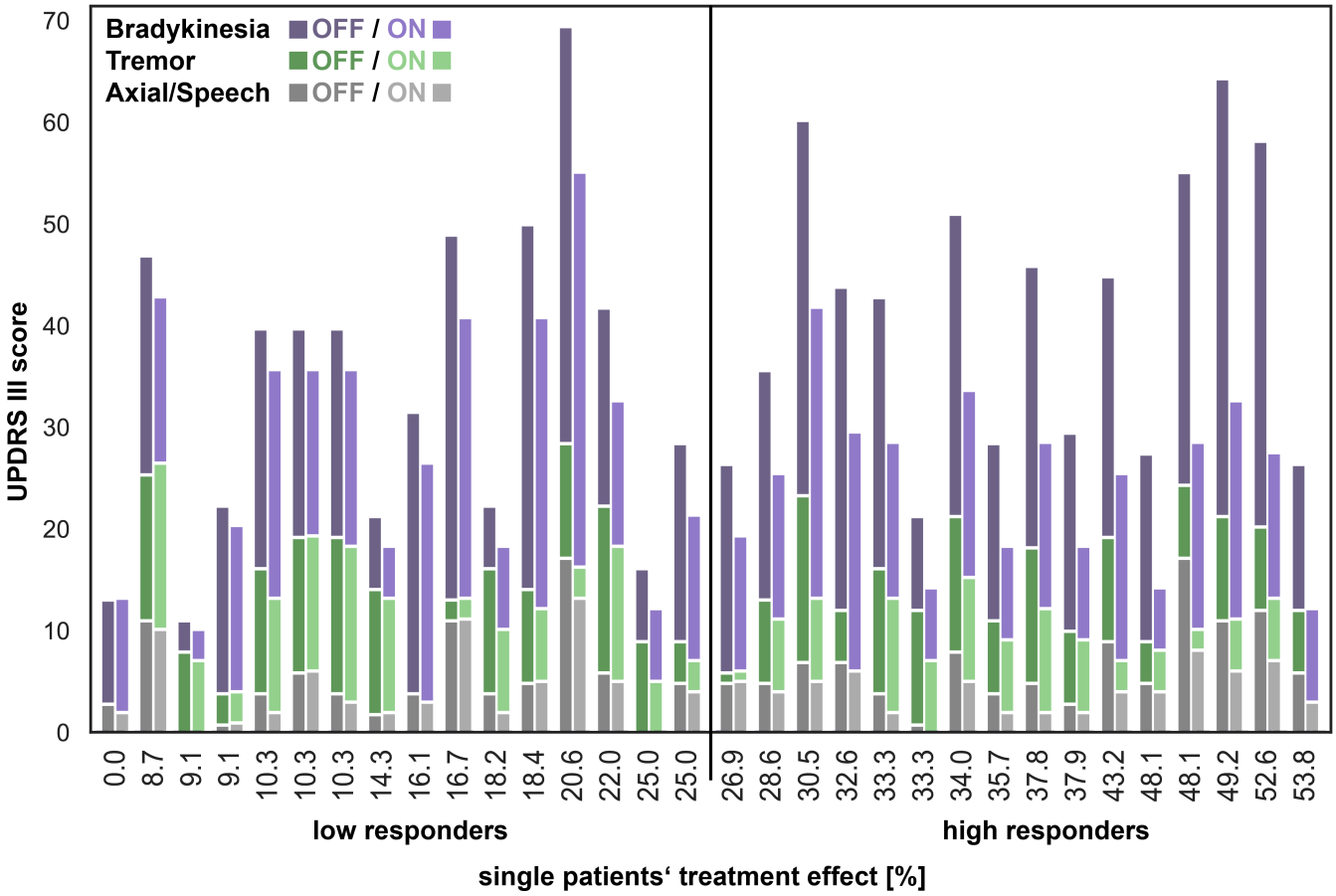
Bradykinesia OFF / ON
Tremor OFF / ON
Axial/Speech OFF / ON
UPDRS III score
0
10
20
30
40
50
60
70
0.0
8.7
9.1
9.1
10.3
10.3
10.3
14.3
16.1
16.7
18.2
18.4
20.6
22.0
25.0
25.0
26.9
28.6
30.5
32.6
33.3
33.3
34.0
35.7
37.8
37.9
43.2
48.1
48.1
49.2
52.6
53.8
low responders
high responders
single patients‘ treatment effect [%]

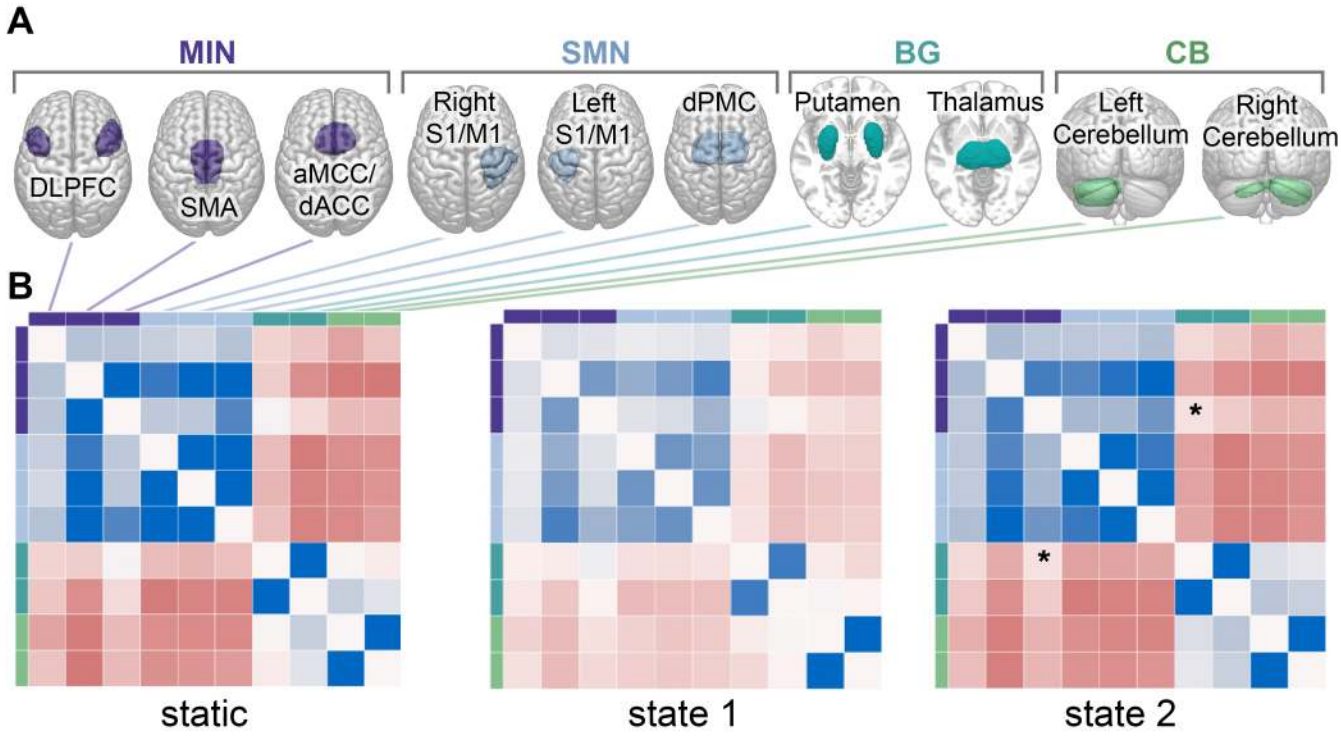
A
MIN
SMN
BG
CB
DLPFC
SMA
aMCC/
dACC
Right
S1/M1
Left
S1/M1
dPMC
Putamen
Thalamus
Left
Cerebellum
Right
Cerebellum
B
*
*
static
state 1
state 2

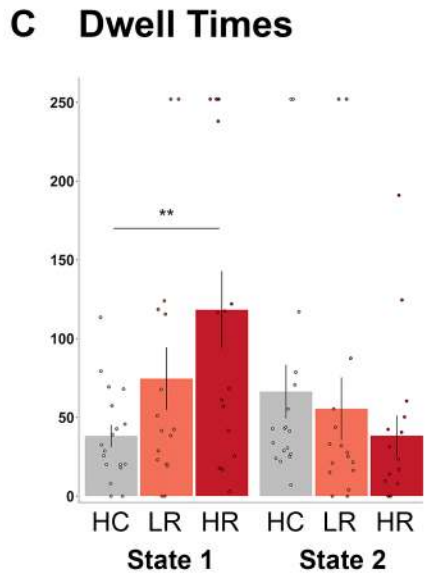
C Dwell Times
250
200
150
100
50
0
**
HC LR HR HC LR HR
State 1
State 2

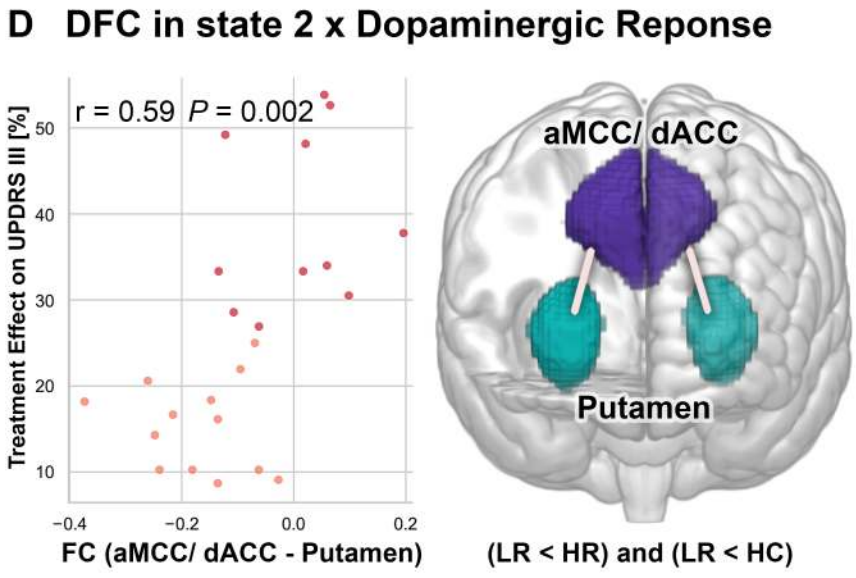
D DFC in state 2 x Dopaminergic Reponse
r = 0.59 P = 0.002
Treatment Effect on UPDRS III [%]
50
40
30
20
10
−0.4
−0.2
0.0
0.2
FC (aMCC/ dACC - Putamen)
aMCC/ dACC
Putamen
(LR < HR) and (LR < HC)

Supplement

Whole-group comparison

Comparing all Patients irrespective of dopaminergic treatment response to healthy controls showed longer dwell times and fraction times of patients in state 1. Detailed results of the t-tests are shown in supplementary table S1.

Table S1:

		HC (n = 18)	**PD (all) (n = 32)**	**P (independent ttest)**
Dwell Time [s]	**State 1**	38.2 ± 29.9	96.5 ± 90.5	**0.011**
	State 2	66.3 ± 72.1	46.8 ± 66.8	0.340
Fraction Time [s]	**State 1**	0.432 ± 0.309	0.634 ± 0.344	**0.044**
	State 2	0.568 ± 0.310	0.366 ± 0.344	**0.044**
Transitions		4.3 ± 2.2	3.3 ± 2.9	0.198

Abbreviations: HC = Healthy Controls, PD = Parkinson's disease Patients

Details on Cognitive Assessment

Table S2:

	HC (n = 18)	PD LR (n = 16)	PD HR (n = 16)	P (ANOVA)
Memory [z]	-0.05 ± 1.03	0.16 ± 0.81	0.04 ± 0.88	0.807
Working memory [z]	0.72 ± 0.67	0.68 ± 0.71	0.27 ± 0.77	0.164
Executive funktion [z]	-0.15 ± 0.96	0.00 ± 0.68	0.37 ± 0.82	0.199
Language [z]	-0.02 ± 0.74	0.39 ± 0.72	0.33 ± 0.69	0.213
Visuospatial [z]	0.36 ± 0.52	0.40 ± 0.65	0.28 ± 0.60	0.851
Global NPT [z]	0.17 ± 0.47	0.33 ± 0.43	0.25 ± 0.46	0.628